Soft x-ray absorption spectroscopy studies of (110) YBa 2 Cu 3 O 6.9 thin film

S. J. Liu, J. Y. Juang, K. H. Wu, T. M. Uen, Y. S. Gou, J. M. Chen, and J.-Y. Lin

Citation: Journal of Applied Physics **93**, 2834 (2003); doi: 10.1063/1.1544072
View online: http://dx.doi.org/10.1063/1.1544072
View Table of Contents: http://scitation.aip.org/content/aip/journal/jap/93/5?ver=pdfcov
Published by the AIP Publishing

Soft x-ray absorption spectroscopy studies of (110) $YBa_2Cu_3O_{6.9}$ thin film

S. J. Liu, J. Y. Juang, K. H. Wu, T. M. Uen, and Y. S. Gou
Department of Electrophysics, National Chiao Tung University, Hsinchu, Taiwan

J. M. Chen[a)]
Synchrotron Radiation Research Center, Hsinchu, Taiwan

J.-Y. Lin
Institute of Physics, National Chiao Tung University, Hsinchu, Taiwan

(Received 25 March 2002; accepted 15 December 2002)

Unoccupied states of the (110) $YBa_2Cu_3O_{6.9}$ (YBCO) thin films were investigated by the $\mathbf{E}\|ab$ and $\mathbf{E}\|c$ polarized O 1*s* x-ray absorption near edge structure (XANES) spectroscopy. With correction of the self-absorption effect, the $\mathbf{E}\|ab$ O 1*s* XANES spectra of the (110) YBCO films obtained from the normal incidence geometry and grazing incidence geometry are very similar. After the self-absorption correction, the $\mathbf{E}\|c$ spectrum of the (110) YBCO film obtained from the normal incidence geometry is almost identical to that of the (001) YBCO film obtained from the grazing incidence geometry. Hole distribution over the different oxygen sites has been derived. The hole number in the apical sites in some thin films obtained in the present investigation is larger than that from the previous x-ray absorption studies of single crystals and from the theoretical calculations. The comparison of the XANES spectra between the (001) and (110) YBCO thin films is also presented. © *2003 American Institute of Physics.* [DOI: 10.1063/1.1544072]

I. INTRODUCTION

It has been well established that one of the key parameters controlling the superconducting transition temperature (T_c) value of the *p*-type superconducting cuprates is the carrier concentration in the CuO_2 planes.[1] T_c as a function of hole concentration in the CuO_2 planes is found to follow a parabolic curve for many hole-doped high-T_c cuprate superconductors.[2] Also several theories for high-T_c cuprates suggest that the apical O $2p_z$ orbital plays an important role on superconductivity.[3–6] For example, the presence of apical oxygen atoms makes the CuO_2 plane easier to dope with holes.[6] The significance of apical O $2p_z$ states in determining the nature and dispersion of quasiparticle states of hole-doped cuprates has been proposed.[7] Also Di Castro *et al.* have explained the depression of T_c above a certain dopant concentration by the occupancy of holes on Cu $3d_{3z^2-r^2}$ and apical O $2p_z$ hybrids.[8] Thus, hole carriers in the apical oxygen sites are proposed to have a negative influence on the superconductivity in the layered cuprates. In contrast, based on the polarization-dependent O 1*s* and Cu 2*p* x-ray absorption measurements on the $Y_{1-x}Ca_xBa_zCu_3O_{7-y}$ single crystals by Merz *et al.*, it was concluded that the maximum achievable T_c in *p*-type cuprates is governed by not only the planar hole concentration but also the number of holes on the apical site.[9] In other words, to obtain the maximum T_c, the optimally doped planes and the optimum hole number in the apical sites are equally important. It is therefore essential to accurately probe the hole count in the apical oxygen sites in the high-T_c cuprates to develop a comprehensive understanding of the superconducting properties.

It is well-known that the x-ray absorption near edge structure (XANES) measurement is a powerful tool to investigate the unoccupied (hole) states in high-T_c cuprates.[9–15] In particular, polarized O *K*-edge XANES spectrum is capable of giving information about the hole carriers on the specific sites. Due to the anisotropy of $YBa_2Cu_3O_{6.9}$ (YBCO), $\mathbf{E}\|ab$ and $\mathbf{E}\|c$ O 1*s* XANES spectra can provide the distribution of hole carriers over the different oxygen sites. **E** represents the electric field vector of the linearly polarized synchrotron light. Knowledge of hole distribution on the different sites is indispensable to investigate the effects of, for example, Ca and Pr substitution in YBCO.[9,10] However, there is a large discrepancy for the hole number in the apical oxygen sites in the YBCO single crystals in the literature (for example, $n_{\text{apex}}=0.2$ in Ref. 16 and $n_{\text{apex}}=0.27$ in Ref. 9).

The in-plane *c*-axis-aligned YBCO thin films exhibit the *c* axis lying in the surface plane and make a longer superconducting coherence length accessible for the fabrication of Josephson tunneling junctions. Due to the significance of fabricating planar tunneling junctions, the growth of the (100) and (110) YBCO thin films has recently attracted great attention. Several groups have successfully grown the (100) and (110) YBCO thin films in spite of containing some impurity phases such as (103).[17] Using the well-oriented (110) YBCO thin film with the *c* axis aligning along the substrate plane, both the $\mathbf{E}\|c$ and $\mathbf{E}\|ab$ absorption spectra can be measured from the normal incidence geometry. Furthermore, in the $\mathbf{E}\|c$ geometry, the $\mathbf{E}\|ab$ spectra can also be obtained by the grazing incidence geometry.

In this study, unoccupied states of the well-oriented (001) and (110) YBCO thin films were investigated by the $\mathbf{E}\|c$ and $\mathbf{E}\|ab$ O 1*s* x-ray absorption spectra. The distribution of hole carriers on the different oxygen sites was mea-

[a)]Electronic mail: jmchen@srrc.gov.tw

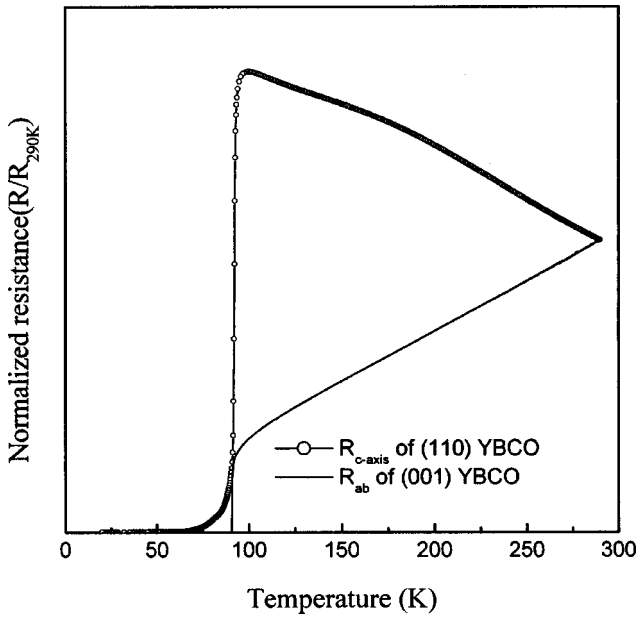

FIG. 1. Normalized resistance ($R/R_{290\,\mathrm{K}}$) vs T of (a) the well-oriented (110) YBCO and (b) (001) YBCO.

sured and compared with results from both the previous x-ray absorption studies of single crystals and theoretical calculations. The comparison of the absorption spectra between the (001) and (110) YBCO thin films related to their superconducting properties is also discussed.

II. EXPERIMENTS

The well-oriented (110) YBCO thin film was deposited on the (110) $SrTiO_3$ surface with the $PrBa_2Cu_3O_{7-y}$ layer as a buffer layer by the pulsed laser deposition (PLD) method. The detailed deposition conditions and the sample characterization will be described elsewhere.[18] The well-oriented (001) YBCO thin film was deposited on (100) $SrTiO_3$ substrate by PLD. The normalized resistance vs. temperature of both samples is shown in Fig. 1. Both samples show decent T_c of 89 K and similar electric transport properties. The thickness of the two films is estimated to be about 3000–4000 Å which is thick enough to avoid the contribution from the buffer layer and the oxide substrate. The x-ray absorption experiments were performed at the high-energy spherical grating monochromator (HSGM) beamline of the Synchrotron Radiation Research Center in Taiwan. The photon energy was calibrated using the known O K-edge absorption peaks of CuO. The energy resolution of the monochromator was set to ~0.2 eV for the O K-edge range. The incident photon flux (I_0) was monitored simultaneously by a Au-coated mesh located after the exit slit of the monochromator. All the absorption measurements were normalized to I_0. Figure 2 shows the geometry arrangements of the incident linearly polarized x-ray and thin films. Figures 2(a) and 2(b) for the $\mathbf{E}\|c$ and $\mathbf{E}\|ab$ geometries correspond to a normal-incident alignment with the polarization vector of incident synchrotron light parallel and perpendicular to the c axis of thin films, respectively. For the $\mathbf{E}\|c$ geometry, the sample

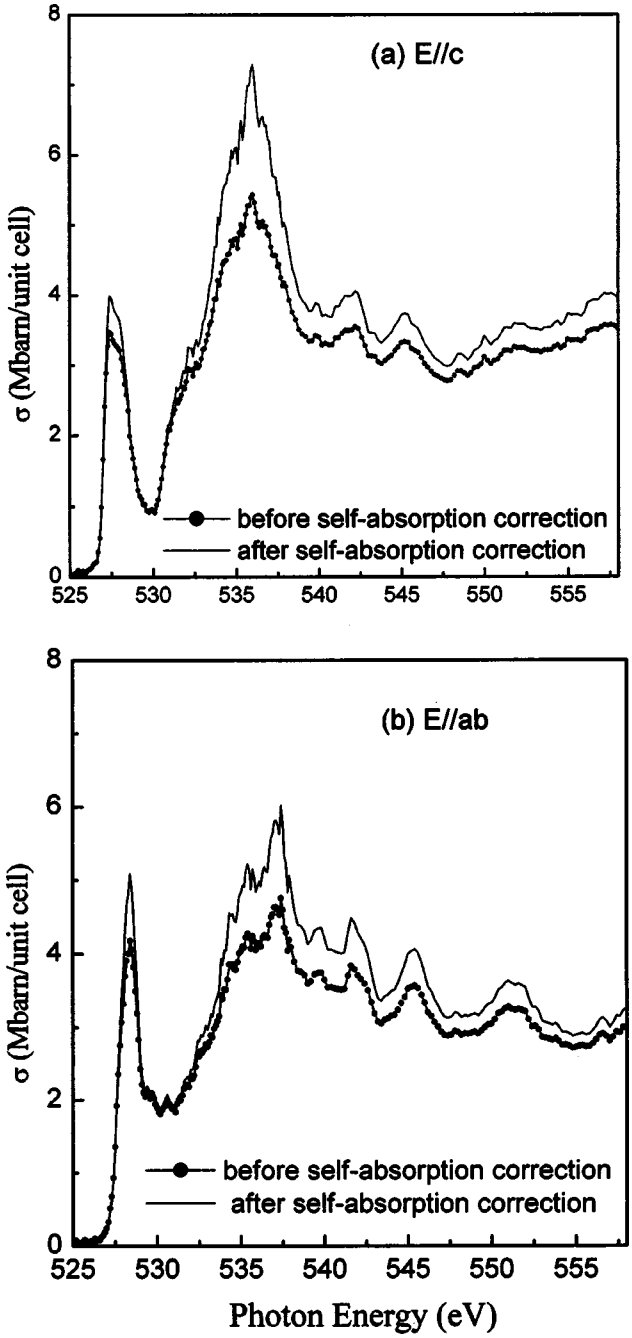

FIG. 3. (a) $\mathbf{E}\|c$ and (b) $\mathbf{E}\|ab$ O 1s XANES spectra of the well-oriented (110) YBCO thin films. The spectra before and after the self-absorption correction are depicted.

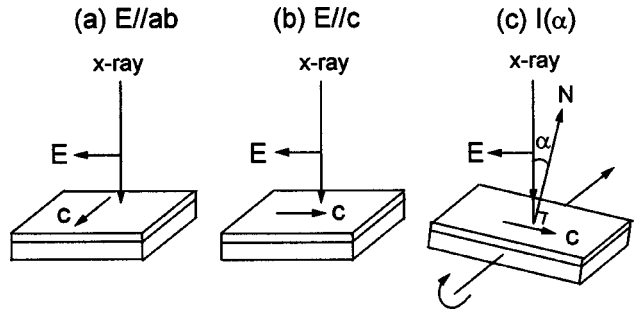

FIG. 2. The geometry arrangement of the incident polarized x-ray and well-oriented (110) YBO thin films for the (a) $\mathbf{E}\|ab$, (b) $\mathbf{E}\|c$, and (c) $I(\alpha)$ spectra, respectively. **E** represents the electric field vector of the linearly polarized synchrotron light.

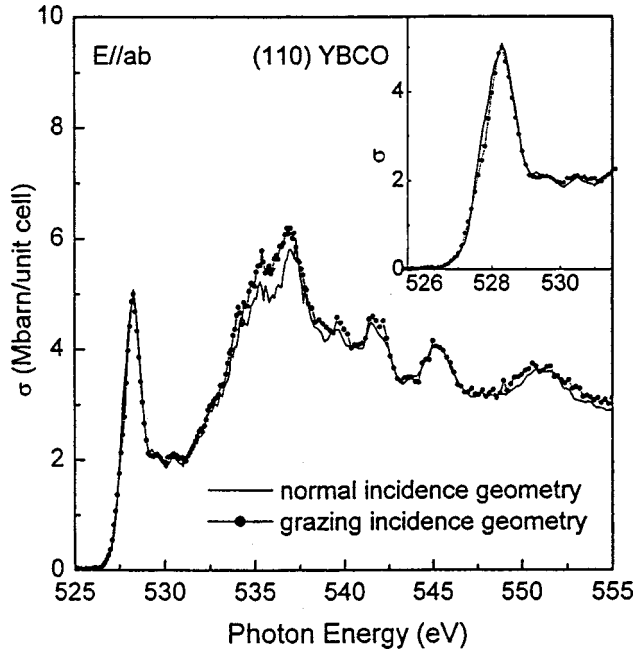

FIG. 4. Comparison of the $\mathbf{E}\|ab$ O 1s XANES spectra of the (110) YBCO thin film obtained from the normal incidence geometry and grazing incidence geometry. The pre-edge spectra are presented in the insets.

was rotated with $\alpha=60°$ and 75° (α is the angle between the incident synchrotron beam and the surface normal) to obtain the polarized x-ray absorption spectra $I(\alpha)$ [Fig. 2(c)]. According to

$$I(\alpha)=I_{\mathbf{E}\|c}\cos^2(\alpha)+I_{\mathbf{E}\|ab}\sin^2(\alpha) \tag{1}$$

the $\mathbf{E}\|ab$ spectra were deduced.

X-ray absorption spectra were recorded by a bulk-sensitive x-ray-fluorescence-yield (XFY) mode. However, for concentrated samples, the XFY spectra exhibit the considerable distortions due to the self-absorption effect. Moreover, these distortions vary with the experimental geometry arrangements and cannot be neglected to obtain the correct absorption spectra. The experimental XFY XANES spectra were corrected for the self-absorption effect by employing[19,20]

$$\frac{I_F(E)}{I_0(E)}\propto\frac{\mu_X(E)}{\dfrac{\mu_{\text{total}}(E)}{\cos\alpha}+\dfrac{\mu_{\text{total}}(E_F)}{\cos\beta}}, \tag{2}$$

where E and E_F are the energy of the incident x ray and the fluorescence, respectively. $I_F(E)$ is the intensity of the fluorescence detected. $I_0(E)$ denotes the intensity of the incoming x ray. $\mu_x(E)$ is the absorption coefficient associated with the production of a core hole in the investigated level X. β is the angle between the sample normal and the outgoing fluorescence toward the detector. $\mu_{\text{total}}(E)$ denotes the absorption coefficients of all elements in the sample. The spectra were normalized to the tabulated standard absorption cross section[21] in the energy range from 600 to 620 eV. The axis of the fluorescence detector was oriented at 45° with respect to the incident photon beam. In this geometry, for $\alpha=60°$ and 75°, $\beta=15°$ and 30°, respectively. The x-ray absorption measurements were performed at room temperature.

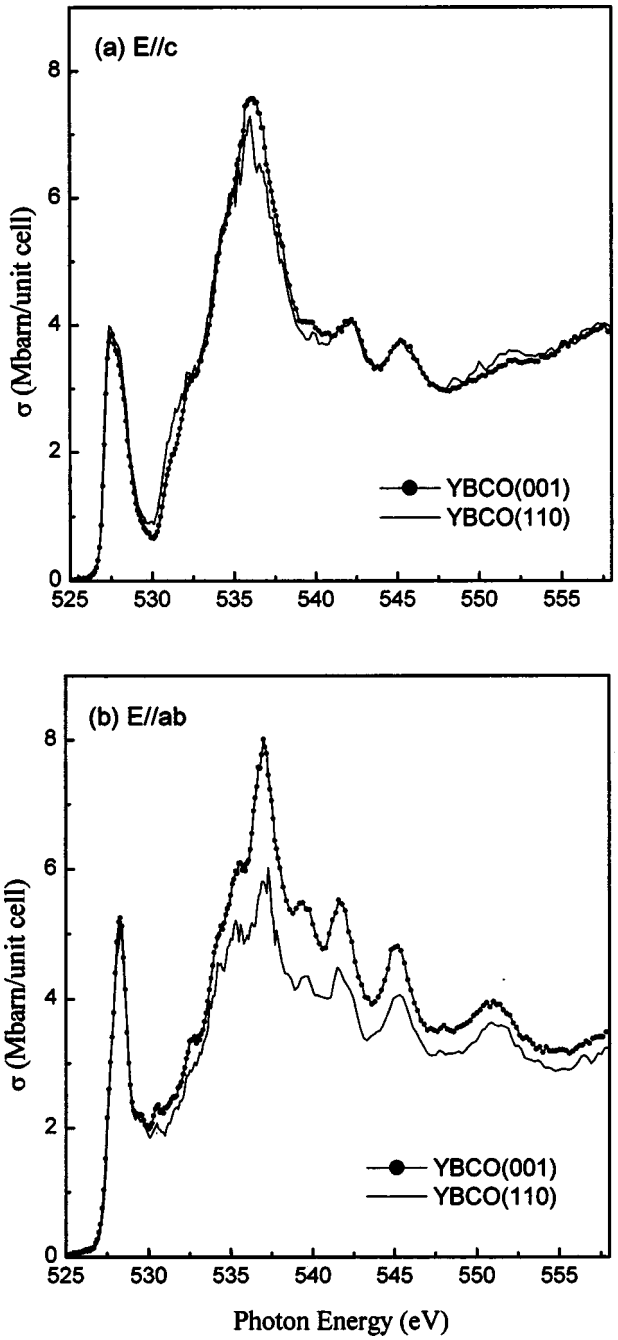

FIG. 5. (a) Comparison of the $\mathbf{E}\|c$ spectrum of the (110) YBCO thin film measured from the normal incidence geometry and the $\mathbf{E}\|c$ spectrum of the (001) YBCO film obtained from the grazing incidence geometry. (b) $\mathbf{E}\|ab$ O 1s XANES spectra of the (001) and (110) YBCO.

III. RESULTS AND DISCUSSION

In Fig. 3, the $\mathbf{E}\|c$ and $\mathbf{E}\|ab$ O 1s XANES spectra of the (110) YBCO thin film obtained from the normal incidence geometry are reproduced before and after the self-absorption correction. The absorption features of the $SrTiO_3$ substrate are not observed in Fig. 3, as demonstrated in Ref. 22. This ensures that the observed spectra reflect only the bulk properties of YBCO. As shown in Fig. 3(a), the pre-edge peak at ~528 eV in the $\mathbf{E}\|c$ spectrum of the (110) YBCO thin film is assigned to the O $2p_z$ hole states in the apical oxygen sites. For the $\mathbf{E}\|ab$ spectra in Fig. 3(b), the absorption feature at

~528.4 eV is ascribed to the hole states in the CuO_2 plane (i.e., the Zhang–Rice states), while the shoulder at ~527.8 eV corresponds to the unoccupied states in the CuO chain.[1,9] The peak at ~529.5 eV is associated with the upper Hubbard band. It is clearly seen from Fig. 3 that the distortion of the XFY spectra due to the self-absorption effect cannot be ignored. Thus, the self-absorption correction is crucial for quantitative analyses to obtain the number of hole carriers on the specific sites.

Figure 4 presents the $\mathbf{E}\|ab$ O 1*s* XANES spectra of the (110) YBCO thin film obtained from the normal incidence geometry [in Fig. 2(a) geometry] and grazing incidence geometry [in Fig. 2(c) geometry]. As noted, after correction of the self-absorption effect, the XFY spectra obtained from different incident geometries become much closer to each other, while the pre-edge region shows only a slight difference, as shown in inset of Fig. 4(a). This clearly confirms that the technique of the self-absorption correction can be successfully used for complex XANES spectra of high-T_c cuprates.

In Fig. 5(a), the $\mathbf{E}\|c$ O *K*-edge XANES spectra of both the (110) and (001) YBCO thin films are depicted. The former is measured from the normal incidence geometry, while the latter is obtained from the grazing incidence geometry. As noted, after the self-absorption correction, the $\mathbf{E}\|c$ spectra of both thin films with different orientations are almost the same, although the pre-edge region shows a slight difference. In general, the purity of the (110) thin films cannot reach 100%.[19] The (103) impurity phase could lead to a difference in the $\mathbf{E}\|c$ spectra of both films with different orientations. The similarity of the $\mathbf{E}\|c$ spectra of the (001) and (110) thin films infers that the (110) YBCO thin film we prepared is rather pure with respect to the orientation. Figure 5(b) shows the $\mathbf{E}\|ab$ O *K*-edge XANES spectra of both the well-oriented (001) and (110) YBCO thin films obtained from the normal incidence geometry. As noted, there is a small difference in the $\mathbf{E}\|ab$ spectra of the (001) and (110) YBCO thin films for the energy range above the edge, while the pre-edge region of these two films is very similar. Although hole number in the apical sites of the (001) and (110) YBCO thin films shows a slight difference [see Fig. 5(a)], planar hole concentration for both films is almost identical [see Fig. 5(b)]. T_c is considered to be determined predominantly by the hole number in the CuO_2 planes. Accordingly, the similarity of the pre-edge $\mathbf{E}\|ab$ spectra of two thin films is associated with their nearly identical T_c's as shown in Fig. 1.

The hole number on the different oxygen sites of the (001) and (110) YBCO thin films, derived from the integrated cross section of the pre-edge absorption peaks, is listed in Table I. The hole fractions were compared with those from the previous XANES studies of single crystals as well as calculated values and results from the nuclear magnetic resonance (NMR) investigations coupled with electrical-field gradient calculations,[23] as listed in Table I. $2n_{ab}$ and n_{chain}, obtained from the O 1*s* $\mathbf{E}\|ab$ XANES spectra, represent the total amount of holes in the CuO_2 planes and in the CuO chains, respectively. Due to the randomness of the *a* and *b* axis arrangement of the YBCO thin film, unlike the single crystal, the contribution from the O(2) and O(3) in the CuO_2 planes cannot be distinguished. n_{apex}, obtained from the $\mathbf{E}\|c$ XANES spectra, corresponds to the hole content in the apical O sites. n_{total} is the total hole number of all the O sites in an unit cell. The total hole number per unit cell is assumed to be 0.9, since the oxygen content of the two YBCO thin films under studied is estimated to be 6.9. As noted from Table I, the hole number in the apical sites in the present investigation is sometimes larger than that from the previous x-ray absorption studies of single crystals (Ref. 16) and from the theoretical calculations. Within the errors, the values of n_{apex} for (001) thin film (our work) and Ref. 9 are in good agreement. However, the n_{apex} value of the (110) YBCO film (our work) is larger than one obtained from recent XANES studies in the YBCO single crystals (Ref. 9). Since the number of apical holes in some YBCO films is larger than those in single crystals, in principle this difference could manifest itself in properties such as anisotropy and interlayer coupling. Further investigations of *c*-axis transport and optical properties in the YBCO thin films are desirable.[24] On the other hand, the $2n_{ab}$ values of two films are slightly smaller than one in single crystals. As expected, the T_c (~89 K) of thin films is slightly smaller than that of single crystals (~92 K). The T_c deviations between present thin films and single crystals may be due to the variations in

TABLE I. Hole distribution on the different oxygen sites of the well-oriented (001) and (110) YBCO thin films as obtained by present experiments. Hole number, n_{ab} and n_{chain}, are analyzed by fitting the E//*ab* XANES spectra to a sum of Gaussian. n_{apex} is obtained from the **E**//*c* XANES spectra. For comparison, the results of previous XANES measurements by Merz *et al.* (XASI) (Ref. 9), Nücker *et al.* (XAS2) (Ref. 1), Krol *et al.*, (XAS3) (Ref. 16), of band-structure calculations (BSC) (Ref. 25), of calculations using three-band model (3BM) with local-density approximation (Ref. 26), and NMR results coupled with calculations of the electric-field gradients (EFG) (Ref. 23) are listed. Estimated error for the *n* values ±0.02. The oxygen content (O_{total}) for different samples is included.

Site	110[a]	001[b]	XAS1	XAS2	XAS3	BSC	3BM	EFG
n_{chain}	0.19	0.21	0.24	0.34	0.27	0.17	0.22	0.30
$2n_{\text{ab}}$	0.38	0.39	0.40	0.40	0.52	0.60	0.76	0.50
n_{apex}	0.33	0.30	0.27	0.26	0.20	0.20	0.24	0.28
n_{total}	0.90	0.90	0.91	1.00	0.99			
O_{total}	6.90	6.90	6.91	7.0	6.99			

[a](110) YBCO.
[b](001) YBCO.

the crystal/film growth processes. However, the overall quantitative consistency of hole distribution and the similarity of the absorption spectra between the epitaxial thin films (this work) and single crystals (Ref. 9) are especially noteworthy. This suggests that the similar XANES studies can be conducted using the high-quality epitaxial thin films, which in some cases are more convenient to fabricate.

IV. CONCLUSION

In conclusion, using the (110) YBCO thin film, the $\mathbf{E}\|c$ O 1*s* XANES spectra of YBCO was measured from the normal incidence geometry. With correction of self-absorption effect, the $\mathbf{E}\|ab$ O 1*s* XANES spectra of the same (110) film obtained from the normal incidence and grazing incidence geometries are very similar. After the self-absorption correction, the $\mathbf{E}\|c$ spectrum of (110) YBCO thin film measured from the normal incidence geometry is almost identical to that of the (001) YBCO films obtained from the grazing incidence geometry. Hole distribution over the different oxygen sites on the (001) and (110) YBCO thin films has been derived. The hole number in the apical sites in some films obtained in the present investigation is larger than that obtained from the previous XANES studies of single crystals and from the theoretical calculations.

[1] N. Nücker *et al.*, Phys. Rev. B **51**, 8529 (1995).
[2] J. L. Tallon, C. Bernhard, H. Shaked, R. L. Hitterman, and J. D. Jorgensen, Phys. Rev. B **51**, 12911 (1995).
[3] E. Kaldis, P. Fischer, A. W. Hewat, E. A. Hewat, J. Karpinski, and S. Rusiecki, Physica C **159**, 668 (1989).
[4] C. Murayama, N. Môri, S. Yomo, H. Takagi, S. Uchida, and Y. Tokura, Nature (London) **339**, 293 (1989).
[5] H. Matsukawa and H. Fukuyama, J. Phys. Soc. Jpn. **59**, 1723 (1990).
[6] J. B. Torrance *et al.*, Phys. Rev. B **40**, 8872 (1989).
[7] J. B. Grant and A. K. McMahan, Phys. Rev. B **46**, 8840 (1990).
[8] C. Di Castra, L. F. Feiner, and M. Gilli, Phys. Rev. Lett. **66**, 3209 (1991).
[9] M. Merz *et al.*, Phys. Rev. Lett. **80**, 5192 (1998).
[10] M. Merz *et al.*, Phys. Rev. B **55**, 9160 (1997).
[11] J. M. Chen, R. S. Liu, J. G. Lin, C. Y. Huang, and J. C. Ho, Phys. Rev. B **55**, 14586 (1997).
[12] E. Pellegrin *et al.*, Phys. Rev. B **47**, 3354 (1993).
[13] C. T. Chen, L. H. Tjeng, J. Kwo, H. L. Kao, P. Rudolf, F. Sette, and R. M. Fleming, Phys. Rev. Lett. **69**, 2543 (1992).
[14] J.-H. Park, C. T. Chen, S.-W. Cheong, W. Bao, G. Meigs, V. Chakarian, and Y. U. Idzerda, Phys. Rev. Lett. **76**, 4215 (1996).
[15] D. D. Sarma, O. Rader, T. Kachel, A. Chainani, M. Mathew, K. Holldack, W. Gudat, and W. Eberhardt, Phys. Rev. B **49**, 14238 (1994).
[16] A. Krol *et al.*, Phys. Rev. B **45**, 2581 (1995).
[17] For examples, S. Misat, P. J. King, D. Fuchs, J. C. Villegier, R. P. Campion, and P. S. Czerwinka, Physica C **331**, 241 (2000).
[18] S. P. Chen, J. Y. Juang, K. H. Wu, T. M. Uen, Y. S. Gou (unpublished).
[19] L. Tröger, D. Arvanitis, K. Baberschke, H. Michaelis, U. Grimm, and E. Zschech, Phys. Rev. B **46**, 3283 (1992).
[20] C. H. Booth, F. Bridges, J. B. Boyce, T. Claeson, B. M. Lairson, R. Liang, and D. A. Bonn, Phys. Rev. B **54**, 9542 (1996).
[21] J. J. Yeh and I. Lindau, At. Data Nucl. Data Tables **32**, 1 (1995).
[22] S. Gerhold, C. A. Kuntscher, M. Merz, N. Nücker, S. Schupper, W. H. Tang, and J. Gao, Phys. Status Solidi B **215**, 578 (1999).
[23] H. Alloul, T. Ohno, and P. Mendels, Phys. Rev. Lett. **63**, 1700 (1989).
[24] S. L. Cooper and K. E. Gray, in *Physical Properties of High Temperature Superconductors*, edited by D. M. Ginsberg (World Scientific, Singapore, 1983), Vol. 4, p. 61.
[25] W. M. Temmerman, Z. Szotec, and G. Y. Guo, J. Phys. C **21**, L867 (1988).
[26] A. M. Olés and W. Grzelka, Phys. Rev. B **44**, 9531 (1991).